CHARLES UNIVERSITY PRAGUE

faculty of mathematics and physics

# Shell galaxies:

## kinematical signature of shells, satellite galaxy disruption and dynamical friction

Summary of Doctoral Thesis

**Ivana Ebrová**

Supervisor: RNDr. Bruno Jungwiert, Ph.D.

Branch: Theoretical Physics, Astronomy and Astrophysics

Prague 2013

This doctoral thesis was done at the Astronomical Institute of the Academy of Sciences of the Czech Republic, v.v.i., during doctoral studies at the Faculty of Mathematics and Physics, Charles University in Prague in the years 2007-2013.


| | |
|---|---|
| PhD student: | Mgr. Ivana Ebrová |
| Supervising workspace: | Astronomický ústav AV ČR<br>Boční II 1401<br>141 31 Praha 4 |
| Supervisor: | RNDr. Bruno Jungwiert, Ph.D.<br>Astronomický ústav AV ČR<br>Boční II 1401<br>141 31 Praha 4 |
| Referees: | RNDr. Ladislav Šubr, Ph.D.<br>Astronomický ústav UK<br>V Holešovičkách 2<br>180 00 Praha 8 |
| | doc. RNDr. Martin Šolc, CSc.<br>Astronomický ústav UK<br>V Holešovičkách 2<br>180 00 Praha 8 |



This summary was distributed on 5. 10. 2013.

The defense is held on 5. 11. 2013 at 14.00 in front of the committee of the study branch 4F1 *Theoretical physics, astronomy and astrophysics* at MFF UK, Ke Karlovu 3, 121 16 Prague 2, Czech Republic, room No. M252.

The thesis is at disposal in the Department of doctoral studies of Faculty of Mathematics and Physics, Charles University in Prague, Ke Karlovu 3, 121 16 Prague 2, Czech Republic and at galaxy.asu.cas.cz/∼ivaana/phd

CHARLES UNIVERSITY PRAGUE
faculty of mathematics and physics

# Galaxie se slupkami:

## kinematika slupek, rozpad satelitní galaxie a dynamické tření

Autoreferát doktorské práce

**Ivana Ebrová**

Školitel: RNDr. Bruno Jungwiert, Ph.D.

Studijní obor: Teoretická fyzika, astronomie a astrofyzika

Praha 2013

Tato disertační práce byla vypracována v Astronomickém ústavu AV ČR, v.v.i., v rámci doktorského studia na Matematicko-fyzikální fakultě Univerzity Karlovy v Praze v letech 2007-2013.


| | |
|---|---|
| Doktorand: | Mgr. Ivana Ebrová |
| Školící pracoviště: | Astronomický ústav AV ČR<br>Boční II 1401<br>141 31 Praha 4 |
| Školitel: | RNDr. Bruno Jungwiert, Ph.D.<br>Astronomický ústav AV ČR<br>Boční II 1401<br>141 31 Praha 4 |
| Oponenti: | RNDr. Ladislav Šubr, Ph.D.<br>Astronomický ústav UK<br>V Holešovičkách 2<br>180 00 Praha 8 |
| | doc. RNDr. Martin Šolc, CSc.<br>Astronomický ústav UK<br>V Holešovičkách 2<br>180 00 Praha 8 |



Autoreferát byl rozeslán dne 5. 10. 2013.

Obhajoba se koná dne 5. 11. 2013 v 14:00 před komisí obhajoby doktorských disertačních prací oboru 4F1 *Teoretická fyzika, astronomie a astrofyzika* na MFF UK, Ke Karlovu 3, 121 16 Praha 2, v místnosti č. M252.

S disertací je možno se seznámit na studijním oddělení doktorské studium MFF UK, Ke Karlovu 3, 121 16 Praha 2 nebo v elektronické verzi na adrese galaxy.asu.cas.cz/∼ivaana/phd

# Contents



## Acknowledgements

We acknowledge support from the following sources: grant No. 205/08/H005 by Czech Science Foundation; research plan AV0Z10030501 by Academy of Sciences of the Czech Republic; and the project SVV-265301 by Charles University in Prague. This work has been done with the support for a long-term development of the research institution RVO67985815.

# 1 Objectives and motivation

The most successful theory of the evolution of the Universe so far seems to be the theory of the hierarchical formation based on the assumption of the existence of cold dark matter, significantly dominating the baryonic one. In such a universe, large galaxies are formed by merging of small galaxies, protogalaxies and diffuse accretion of surrounding matter. Galactic interaction and dark matter play thus a crucial role in the life of every galaxy.

But the determination of both the dark matter content and the merger history of a galaxy is difficult. Firstly, the cold dark matter interacts only gravitationally (and possibly via the weak interaction) and thus the mapping of its distribution in galaxies is tricky. Secondly, the nature disallows us to see individual galaxies from different angles, thus our knowledge of their spatial properties is degenerated. Thirdly, it is non-trivial to determine anything about the history of a given galaxy as the whole existence of humanity presents only a snapshot in the evolution of the Universe. Yet this knowledge is important to confirm or disprove theories of the creation and evolution of the Universe, improve their accuracy and to understand how the Universe we live in actually looks. The deal of the galactic astronomy is to try to circumvent these obstacles.

The issue of the determination of the overall potential and distribution of the dark matter in galaxies is among the most prominent in galactic astrophysics. In disk galaxies, where stars and gas move on near-circular orbits, we can derive the potential (at least in the disk plane) directly up to several tens of kiloparsecs from the center of the galaxy. Early-type galaxies lack such kinematical beacons. Several different methods have been used, including strong gravitational lensing (e.g., Koopmans et al., 2006, 2009; Auger et al., 2010), weak gravitational lensing (e.g., Mandelbaum et al., 2008), X-ray observations of hot gas in the massive gas-rich galaxies (e.g., Fukazawa et al., 2006; Churazov et al., 2008; Das et al., 2010), rotational curves from detected disks and rings of neutral hydrogen (e.g., Weijmans et al., 2008), stellar-dynamical modeling from integrated light spectra (e.g., Thomas et al., 2011), as well using tracers such as planetary nebulae (e.g., Coccato et al., 2009), globular clusters (e.g., Norris et al., 2012) and satellite galaxies (e.g., Nierenberg et al., 2011; Deason et al., 2012). All the methods have various limits. While comparing independent techniques for the same objects at the similar galactocentric radii, the discrepancies in the estimated circular velocity curves were revealed together with several interpretations (e.g., Churazov et al., 2010; Das et al., 2010). The compared techniques usually employ modeling the X-ray emission of the hot gas (assuming hydrostatic equilibrium) and dynamical modeling of the optical data in the massive early-type galaxies. Therefore, even for the most massive galaxies with X-ray observations at disposal, there is a need for other methods to independently constrain the gravitational potential at various radii.

One of the possibilities is to use tidal features left by the galactic interactions. They act as dynamical tracers of the potential of their host galaxies and as hints left behind by the accreted galaxies in the past. The special case is that of arc-like fine

structures found in shell galaxies. Their unique kinematics carries both qualitative and quantitative information on the distribution of the dark matter, the shape of the potential of the host galaxy and its merger history. Moreover, shell galaxies have their own mysteries that call for an explanation.

However all the information is hidden so deep in the structure and kinematics of shell galaxies that it is not clear that they could be practically unraveled. Certainly, a lot of effort and invention is required. In this work we focus mainly on the possibility to deduce the potential of the host galaxy using shell kinematics. We aim at creating equations and algorithms applicable to observed data. Having no such data at hand, we apply these methods to simulated data. All the shells in one galaxy are probably bound by common origin in radial minor merger. Reproducing their overall structure is nevertheless complicated by physical process such as the dynamical friction and the gradual decay of the cannibalized galaxy.

Attempts to date a merger from observed positions of shells have been made in previous works. Recently, Canalizo et al. (2007) presented HST/ACS observations of spectacular shells in a quasar host galaxy and, by simulating the position of the outermost shell by means of restricted $N$-body simulations, attempted to put constraints on the age of the merger. They concluded that it occurred a few hundred Myr to $\sim 2\,\mathrm{Gyr}$ ago, supporting a potential causal connection between the merger, the post-starburst ages in nuclear stellar populations, and the quasar. A typical delay of 1–2.5 Gyr between a merger and the onset of quasar activity is suggested by both $N$-body simulations Springel et al. (2005) and observations Ryan et al. (2008). It might therefore appear reassuring to find a similar time lag between the merger event and the quasar ignition in a study of an individual spectacular object. The issue here is that noone has studied in detail the effects assumed to complicate the shell distribution (the dynamical friction and the gradual decay of the secondary galaxy) and thus it is not clear how exactly they change the shell structure and how they influence the position of the outermost shell. We explore the options for inclusion of the dynamical friction and the gradual decay of the cannibalized galaxy in test-particle simulations and we look at what these simulations tell us about the potential and merger history of shell galaxies.

Self-consistent simulations allow us to simulate many physical processes at once. Some of them are difficult or outright impossible to reproduce by analytical or semi-analytical methods. At the same time, the manifestation of these processes in self-consistent simulations is difficult to separate and sometimes they may even be confused with non-physical outcomes of used methods. Moreover, self-consistent simulations with high resolution necessary to analyze delicate tidal structures such as the shells are demanding on computation time. This demand is even larger if we are to explore a significant part of the parameter space. In this study, we focus mainly on test-particle simulations and analytical approaches. The doctoral thesis; this summary of the thesis; and videos, mostly illustrating the formation and evolution of shell structures, can be downloaded at: galaxy.asu.cas.cz/∼ivaana/phd

## 2 Shell galaxies in brief

Shell galaxies, like e.g. the beautiful and renowned NGC 3923 in Fig. 1, are galaxies containing ring-like fine structures. These structures are made of stars and form open, concentric arcs that do not cross each other. The term *shells* has spread throughout the literature, gradually superseding the competing term *ripples*. According to the knowledge gained over the past more than twenty years, their origin lies in the interactions between galaxies.

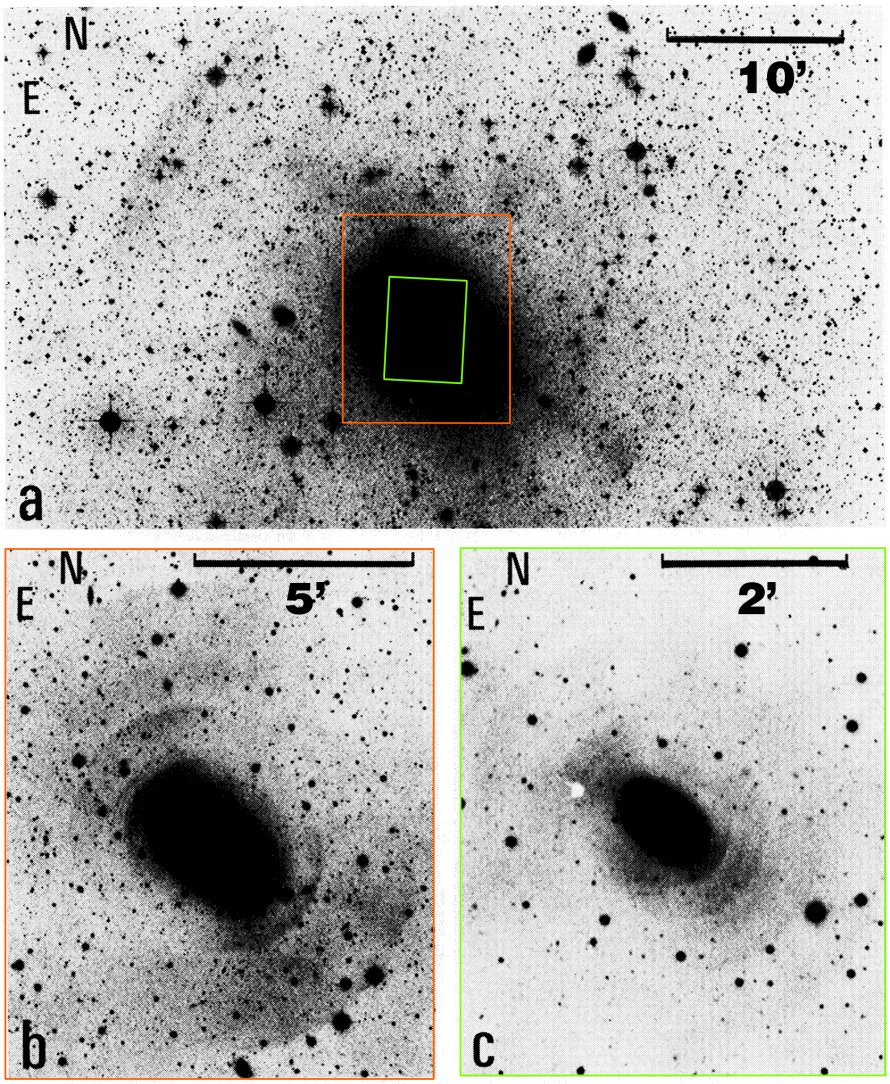


Figure 1: NGC 3923 from Malin & Carter (1983) made from UK Shmidt IIIa-J plates. The bottom row shows more central parts of the galaxy. All images were processed (unsharp masking) to emphasize the shell structure. 10″ roughly corresponds to 1 kpc in the galaxy.

# 3 Observational knowledge of shell galaxies

It was also Halton Arp, who first noticed the shell galaxies in his Atlas of Peculiar Galaxies (Arp, 1966a) and the accompanying article Arp (1966b). To date, the only (at least partial, 137 galaxies with declination south of $-17°$) list of shell galaxies is "A catalogue of elliptical galaxies with shells" from Malin & Carter (1983). A brief summary of characteristics of shells and host galaxies could be written in 22 points:

1. Shells are observed in ∼10% of early-type galaxies (E and S0) and ∼1% of spirals (Malin & Carter, 1983; Schweizer & Ford, 1985; Schweizer & Seitzer, 1988; Martínez-Delgado et al., 2010; Tal et al., 2009; Kim et al., 2012) and in Fornax dwarf spheroidal galaxy (Coleman et al., 2004).

2. Shell galaxies occur markedly most often in regions of low galaxy density, up to ∼50% of E and S0 galaxies (Malin & Carter, 1983; Colbert et al., 2001; Reduzzi et al., 1996; Schweizer & Ford, 1985).

3. The number of shells in a galaxy ranges from 1 to ∼30 (Malin & Carter, 1983; Schweizer, 1983; Prieur, 1988; Sikkema et al., 2007).

4. The shells contain at most a few per cent of the overall brightness of the galaxy (Prieur, 1988).

5. Surface brightness contrast of the shells is very low, about 0.1–0.2 mag (Carter et al., 1982; Fort et al., 1986; Prieur, 1988; Sikkema et al., 2007).

6. Shells are of stellar nature.

7. One third of shell galaxies has shells interleaved in radius, well-aligned with the major axis of the galaxy, and their separation increases with radius (Prieur, 1990).

8. They are aligned with the galaxy's major axis and slightly elliptical for flattened galaxies, and randomly spread around the galactic center for nearly E0 galaxies (Wilkinson et al., 1987c; Prieur, 1990).

9. The range of shells' radii is typically less then 10 but can reach over 60 (Dupraz & Combes, 1986).

10. Shells commonly occur close to the nucleus (Wilkinson et al., 1987c).

11. In roughly 20% of the systems, the innermost shells have spiral morphology (Wilkinson et al., 1987c).

12. Shells can have any color, perhaps they are rather similar to or slightly redder than the host galaxy (Wilkinson et al., 1987c; Fort et al., 1986; Balcells, 1997; Liu et al., 1999; Pierfederici & Rampazzo, 2004).

13. The colors of shells are different even in the same galaxy, tend to be red in the center and bluer further out (McGaugh & Bothun, 1990; Turnbull et al., 1999; Sikkema et al., 2007).

14. It seems that galaxies with shells also contain central dust features (Sikkema et al., 2007; Rampazzo et al., 2007).

15. An increased amount of dust has been observed in shells (Sikkema et al., 2007).

16. Slightly displaced arcs of H I, with respect to the stellar shells, have been discovered in some galaxies (Schiminovich et al., 1994, 1995; Petric et al., 1997; Schiminovich et al., 1997; Balcells et al., 2001).

17. Molecular gas associated with shells was detected in several galaxies (Charmandaris et al., 2000; Horellou et al., 2001).

18. The detection rate of radio emission of shell galaxies is similar to other early-type galaxies (Wilkinson et al., 1987a).

19. There is probably a strong radio-infrared correlation for galaxies which possess shells (Wilkinson et al., 1987b).

20. 15–20% of shell galaxies have nuclear post-starburst spectra (Carter et al., 1988).

21. There is a strong association between kinematically distinct/decoupled cores and shells in galaxies (Forbes, 1992).

22. Shell galaxies have an enormous diversity of central surface brightness and a wide variety of optical appearances (Wilkinson et al., 1987c,a).

# 4 Scenario of shells origin

The model of a radial merger (Quinn, 1984) seems to be the most successful in reproducing regular shell systems. When a small galaxy (secondary) enters the scope of influence of a big elliptical galaxy (primary) on a radial or close to a radial trajectory, it splits up and its stars begin to oscillate in the potential of the big galaxy which itself remains unaffected. In their turning points, the stars have the slowest speed and thus tend to spend most of the time there, they pile up and produce arc-like structures in the luminosity profile of the host galaxy.

The mechanism is illustrated on the one dimensional example in Fig. 2. The density maxima occur near the turnaround points of the particle orbits. The maximal radial position of the orbit is first reached by the most tightly bound particles, but as more distant particles stop and turn around, the density wave propagates slowly in radius to the outermost turning point set by the least bound particle. The particles

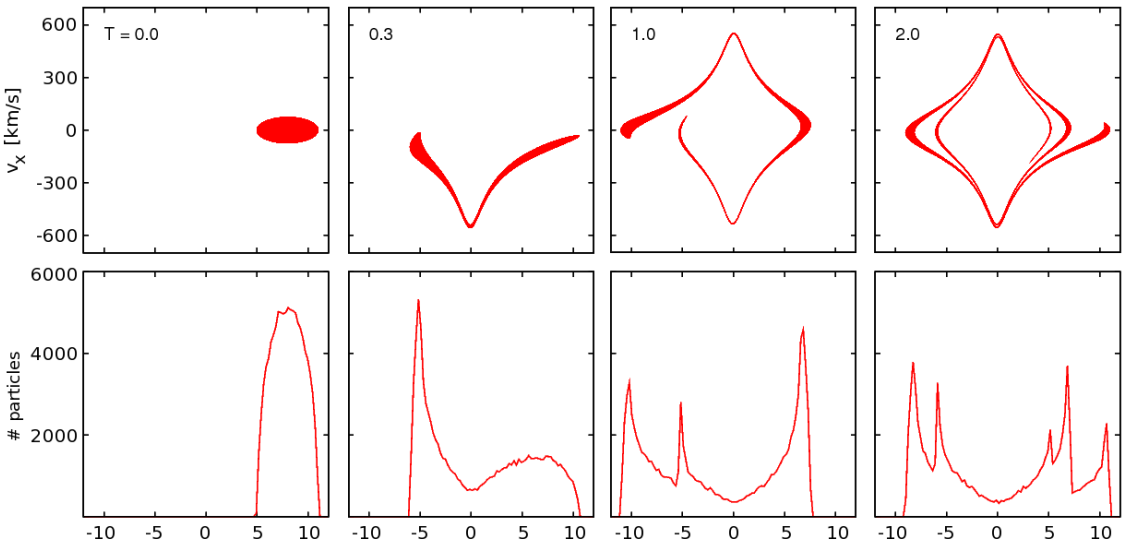


Figure 2: Time evolution of a cloud of test particles falling into a one dimensional plummer potential $v - x$ space (upper row), particle radial density (lower row). The horizontal axis is centered with the center of the potential and scaled so that 1 on the axis is the Plummer radius.

in phase space form a characteristic structure, for which this mechanism of shell formation is often called **"phase wrapping"**.

The edges in density are technically the caustics of the mapping of the phase density of particles into physical space (Nulsen, 1989). As a natural consequence, the shells are interleaved in radius and their separation increases with radius. Furthermore, the range of the number of shells present around ellipticals is a simple consequence of the age of the event. More shells will imply that a longer time has passed since the merger event. In shell galaxies, the shells are traditionally numbered according to the **serial number of the shell**, $n$, from the outermost to the innermost (which in the simple model for a single-generation shell system corresponds to the oldest and the youngest shell, respectively).

# 5 Shell kinematics

A lot of useful information about the shell galaxies can be extracted from the kinematics of the stars forming the shell system. That it is by measuring of the line-of-sight velocity distribution (LOSVD) near the edge of the shell. This idea has been proposed by Merrifield & Kuijken (1998) and we further developed it in the paper Ebrová et al. (2012).

If we approximate the shell system with a simplified model, we can describe its evolution completely depending only on the potential of the host galaxy. The approximation lies in the numerical integration of radial trajectories of stars in a

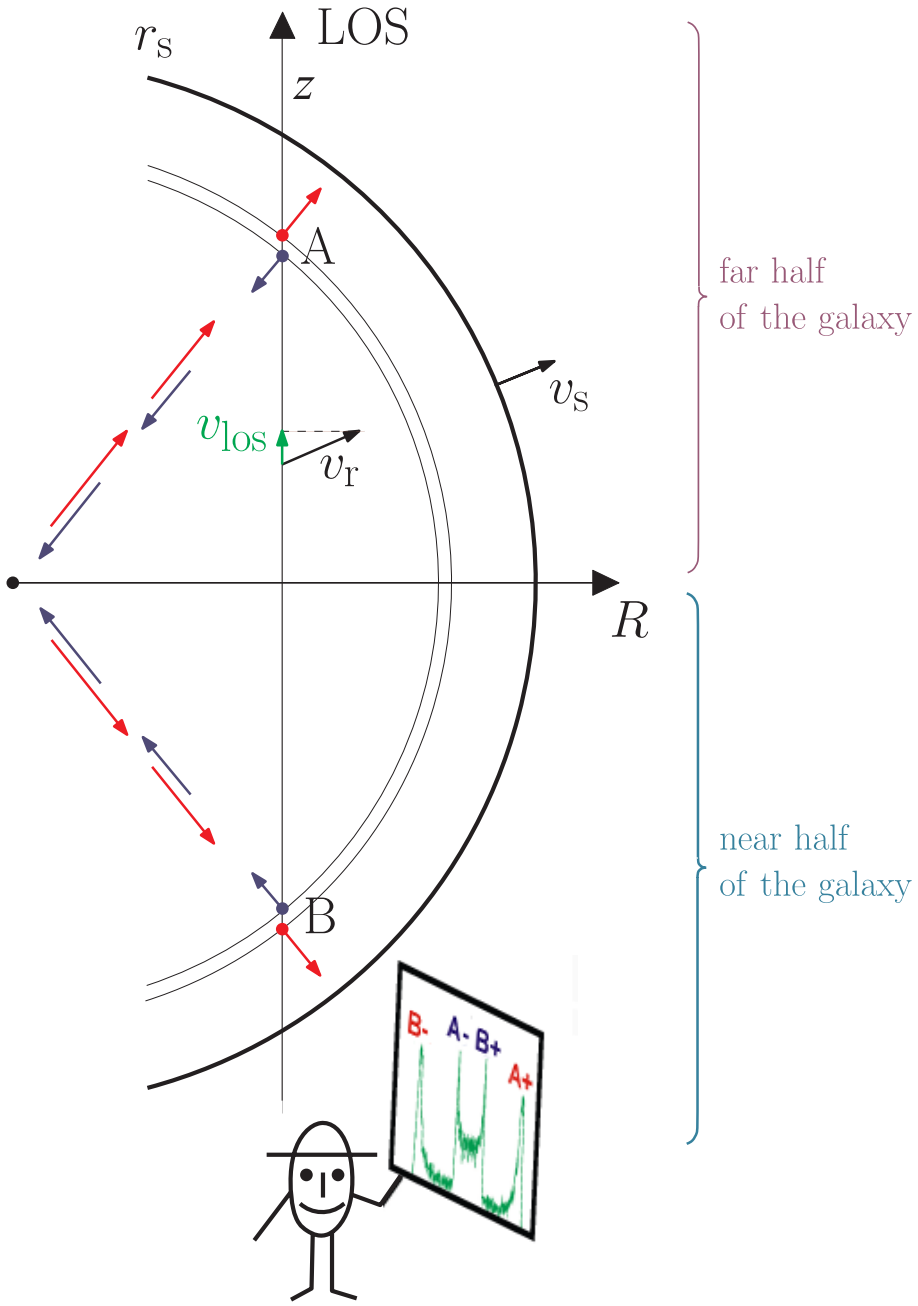


Figure 3: Kinematics of a moving shell. The shell is composed of stars on radial orbits with radial velocity.

spherically symmetric potential. The distribution of energies of stars is continuous, and these stars were released in the center of the host galaxy at the same time.

We call it the **model of radial oscillations**, and it corresponds to the notion that the cannibalized galaxy came along a radial path and disintegrated in the center of the host galaxy. As a result the stars were released at one moment in the center and began to oscillate freely on radial orbits. This approach was first used by

Quinn (1984), followed by Dupraz & Combes (1986, 1987) and Hernquist & Quinn (1987a,b). This model uses the exact knowledge of the chosen potential of the host galaxy, but requires it to be spherically symmetric. The potential can be given analytically or numerically and the stellar trajectories are usually integrated numerically. The main difference from real shell systems is in a very simplified model of the decay of the cannibalized galaxy and the assumption of strictly radial stellar trajectories.

Mr. Eggy measures the LOSVD of stars in the shell, which is composed of inward and outward stars on radial trajectories as illustrated in Fig. 3. The stars near the edge of the shell move slowly. But it is clear from the geometry that contributions add up from different galactocentric distances, where the stars are either still traveling outwards to reach the shell or returning from their apocenters to form the LOSVD at Eggy's picture. For every galactocentric distance intersected by the line of sight, there is a different radial stellar velocity and a different projection factor. The maximal/minimal LOS velocity comes from stars at two particular locations along the line of sight (A and B), both of which are at the same galactocentric distance for outward or inward stars. More precisely, for inward stars, points A and B are a little closer to the center as indicated in Fig. 3.

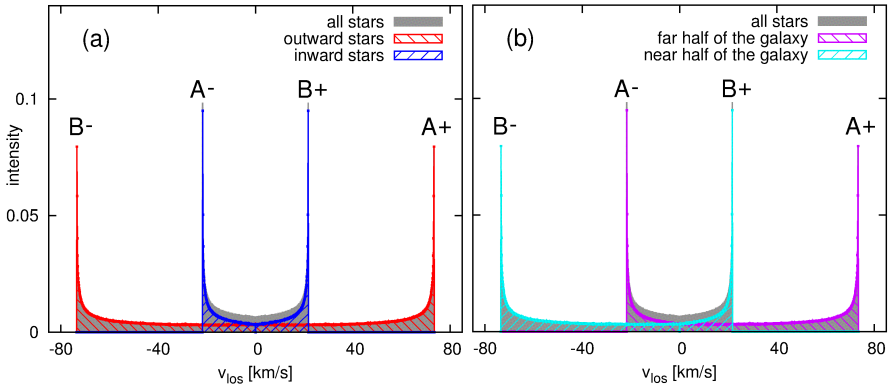


Figure 4: The LOSVD, in the framework of the model of radial oscillations, showing separate contributions from (a) inward and outward stars; (b) the half of the host galaxy closer to the observer (the one including point B) and the more distant half (includes point A). The profile does not include stars of the host galaxy, which are not part of the shell system, and is normalized, so that the total flux equals one.

The edge of the shell moves outwards with velocity $v_s$. At any given instant, the stars that move inwards are returning from a point where the shell edge was at some earlier time, and so their apocenter is inside the current shell radius $r_s$. Similarly, the stars that move outwards will reach the shell edge in the future. Consequently, the stars that move inwards are always closer to their apocenter than those moving outwards at the same radius, and their velocity is thus smaller. The inward stars move toward Mr. Eggy in the farther of the two points (A) and away from them in the nearer point (B), while the stars moving outwards behave in the opposite manner. Together, there are four possible velocities with the maximal contribution

to the LOSVD, resulting in its **symmetrical quadruple shape**. The intensity maxima coincide with velocity extremes for separate contributions to the LOSVD if the distribution is divided into the contribution from near/far half of the galaxy or inward/outward stars, see Fig. 4.

The separation in velocity between peaks for a given projected radius $R$ is given by the distance of $R$ from the edge of the shell. The closer to the shell edge, the narrower the profile is. The separation of the peaks at a given $R$ depends on the phase velocity of the specific shell, near which we observe the LOSVD. This velocity is, for a fixed potential, given by the shell radius and its serial number.

# 6 Constant acceleration and shell velocity

To derive a relation between the shell kinematics and the potential of the host galaxy, we assume following:

- stars were released in the center of the host galaxy at the same time (i.e. strictly radial orbits)
- locally constant value of the radial acceleration $a_0$ in the host galaxy potential[1]
- locally constant[1] velocity of the shell edge $v_\mathrm{s}$
- stars at the shell edge have the same velocity as the shell[2]
- radius of point A and B is equal to $\frac{1}{2}(R + r_\mathrm{s})$

In such an approximation, for the measured locations of the LOSVD peaks $v_{\mathrm{los,max+}}$, $v_{\mathrm{los,max-}}$, projected radius $R$, and shell edge radius $r_\mathrm{s}$, we can express the circular velocity[3] $v_\mathrm{c}$ at the shell edge radius and the current shell velocity $v_\mathrm{s}$ by equations:

$$v_\mathrm{c} = \frac{|v_{\mathrm{los,max+}} - v_{\mathrm{los,max-}}|}{2\sqrt{(1 - R/r_\mathrm{s})\left[1 - 4\left(R/r_\mathrm{s}\right)^2\left(1 + R/r_\mathrm{s}\right)^{-2}\right]}}, \tag{1}$$

$$v_\mathrm{s} = \frac{v_{\mathrm{los,max+}} + v_{\mathrm{los,max-}}}{2\sqrt{1 - 4\left(R/r_\mathrm{s}\right)^2\left(1 + R/r_\mathrm{s}\right)^{-2}}}. \tag{2}$$

[1] By "locally constant" we mean that we apply one constant value of radial acceleration or shell velocity to the calculation of the stellar kinematics for one shell in the whole range of radii of interest.

[2] In fact this is not true but these velocities are very similar

[3] The concept of circular velocity is commonly used even in elliptical galaxies where none or small amount of the matter is expected to move on circular orbits. It is a quantity which says what speed would move the body launched into a circular orbit. Provided spherical symmetry of the galaxy, it simply denotes the quantity $\sqrt{r\phi'(r)}$ , where $\phi'(r)$ is the first derivative of the galactic potential with respect to the galactocentric radius $r$.

Let $\triangle v_{\rm los}$ be the distance between the outer peak for positive velocities and the inner peak for negative velocities or vice versa, $\triangle v_{\rm los} = v_{\rm los,max+} - v_{\rm los,max-}$, then, in the vicinity of the shell edge,

$$\frac{\mathrm{d}\triangle v_{\rm los}}{\mathrm{d}R} \simeq -2\frac{v_{\rm c}}{r_{\rm s}}. \tag{3}$$

This equation allows us to measure the circular velocity in shell galaxies using the **slope of the LOSVD intensity maxima** in the $R \times v_{\rm los}$ diagram. It requires measurements of positions of peaks at two or more different projected radii for the same shell. In exchange it promises a more accurate derivation of $v_{\rm c}$. However it does not allow the derivation of the shell velocity $v_s$. For this purpose, we can derive a **hybrid relation** between the positions of the LOSVD peaks, the circular velocity at the shell edge radius $v_{\rm c}$, and the shell velocity:

$$v_{\rm s}^2 = v_{\rm c}^2(1 - R/r_{\rm s}) + \frac{v_{\rm los,max+}v_{\rm los,max-}}{4\left(R/r_{\rm s}\right)^2\left(1 + R/r_{\rm s}\right)^{-2} - 1}. \tag{4}$$

If we insert the value of $v_{\rm c}$ derived from the measurement of the LOSVD intensity maxima into this equation, we can expect a better estimate of the phase velocity of the shell.

# 7 Test-particle simulation

We performed a simplified simulation of formation of shells in a radial galactic minor merge. Both merging galaxies are represented by smooth potential. Millions of test particles were generated so that they follow the distribution function of the cannibalized galaxy at the beginning of the simulation. The particles then move according to the sum of the gravitational potentials of both galaxies. When the centers of the galaxies pass through each other, the potential of the cannibalized galaxy is suddenly switched off and the particles continue to move only in the fixed potential of the host galaxy. We use the simulation to demonstrate the validity of our methods of recovering the parameters of the host galaxy potential by *measuring*[4] the positions of the peaks in the spectral lines. We look at the galaxy from the view perpendicular to the axis of collision, so that the cannibalized galaxy originally flew in from the right.

The potential of the host galaxy is a double Plummer sphere with respective masses $M_* = 2 \times 10^{11}\,\mathrm{M}_\odot$ and $M_{\rm DM} = 1.2 \times 10^{13}\,\mathrm{M}_\odot$ , and Plummer radii $\varepsilon_* = 5\,\mathrm{kpc}$ and $\varepsilon_{\rm DM} = 100\,\mathrm{kpc}$ for the luminous component and the dark halo, respectively. The potential of the cannibalized galaxy is chosen to be a single Plummer sphere with the total mass $M = 2 \times 10^{10}\,\mathrm{M}_\odot$ and Plummer radius $\varepsilon_* = 2\,\mathrm{kpc}$. The cannibalized galaxy is released from rest at a distance of 100 kpc from the center of the host galaxy. When it reaches the center of the host galaxy in 306.4 Myr, its potential is switched off and its particles begin to oscillate freely in the host galaxy. The shells start appearing visibly from about 50 kpc of galactocentric distance and disappear at

[4]By *measuring,* we mean that the data measured are the output of our simulation.

around 200 kpc, as there are very few particles with apocenters outside these radii, see Fig. 5. Video from the simulation is available at: galaxy.asu.cas.cz/∼ivaana/phd

In the simulations, some of the assumptions that we used earlier (the model of radial oscillations) are not fulfilled. First, the particles do not move radially, but on more general trajectories, which are, even in the case of a radial merger, nevertheless very eccentric. Second, not all the particles are released from the cannibalized galaxy right in the center of the host galaxy; when the potential is switched off, the particles are located in the broad surroundings of the center and some are even released before the decay of the galaxy. These effects cause a smearing of the kinematical imprint of shells, as the turning points are not at a sharply defined radius, but rather in some interval of radii for a given time.

We used a snapshot from our simulation, which 2.2 Gyr after the decay of the cannibalized galaxy, as a source of the simulated data and tried to reconstruct the

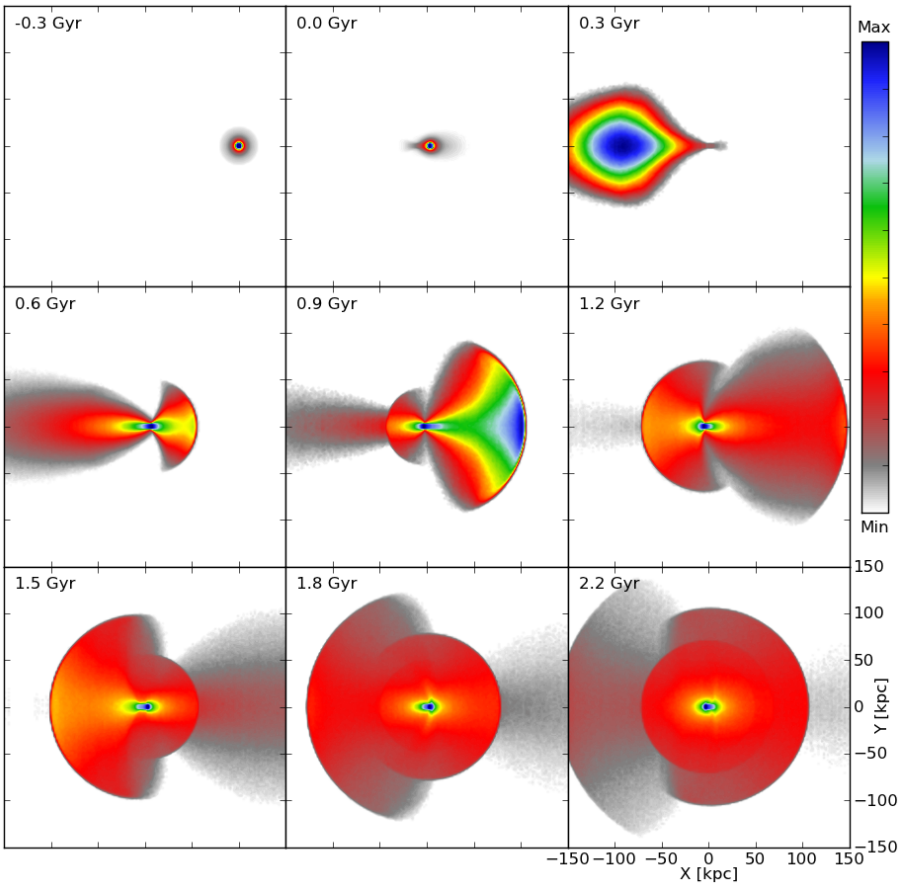


Figure 5: Snapshots from our test-particle simulation of the radial minor merger, leading to the formation of shells. Each panel covers 300×300 kpc and is centered on the host galaxy. Only the surface density of particles originally belonging to the satellite galaxy is displayed. The density scale varies between frames, so that the respective range of densities is optimally covered.

parameters of the potential of the host galaxy from the locations of the LOSVD peaks *measured* from the simulated data by using the the approximation of constant acceleration and shell velocity. The model of radial oscillations predicts that 2.2 Gyr after the decay of the cannibalized galaxy five outermost shells should lie at the radii of 257.3, −157.8, 105.1, −70.5, and 48.8 kpc. The negative radii refer to the shell being on the opposite side of the host galaxy with respect to the direction from which the cannibalized galaxy flew in. These radii agree surprisingly well with the radii of the shells *measured* in the simulation 2.2 Gyr after the decay of the cannibalized galaxy. In the simulation, the first shell at 257.4 kpc is composed of only a few particles, and therefore we will not consider it. Thus, the outermost relevant shell in the system lies at −157.8 kpc and has a serial number $n = 2$. Also, the shell at 48.8 kpc suffers from lack of particles, but we will include it nevertheless. Fig. 6 shows the comparison between the LOSVD in the simulation, the peaks of the LOSVD computed in the model of radial oscillations (light blue curves), and in the approximation of a constant galactic acceleration and shell velocity (orange curves).

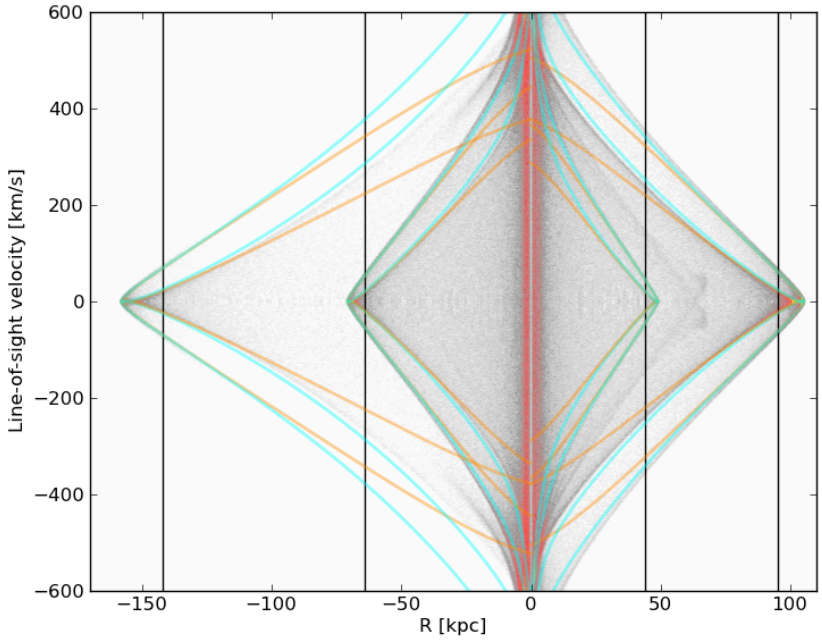


Figure 6: LOSVD map of the simulated shell structure 2.2 Gyr after the decay of the cannibalized galaxy. Black lines mark the location at $0.9r_{\rm s}$ for each shell. The map includes only stars originally belonging to the cannibalized galaxy.

For a given host galaxy, the signal-to-noise (S/N) ratio in the simulated data is a function of the number of simulated particles, the age of the shell system, the distribution function of the cannibalized galaxy, and the impact velocity. For a given radius in the simulated data, we can obtain arbitrarily good or bad S/N ratios by tuning these parameters.

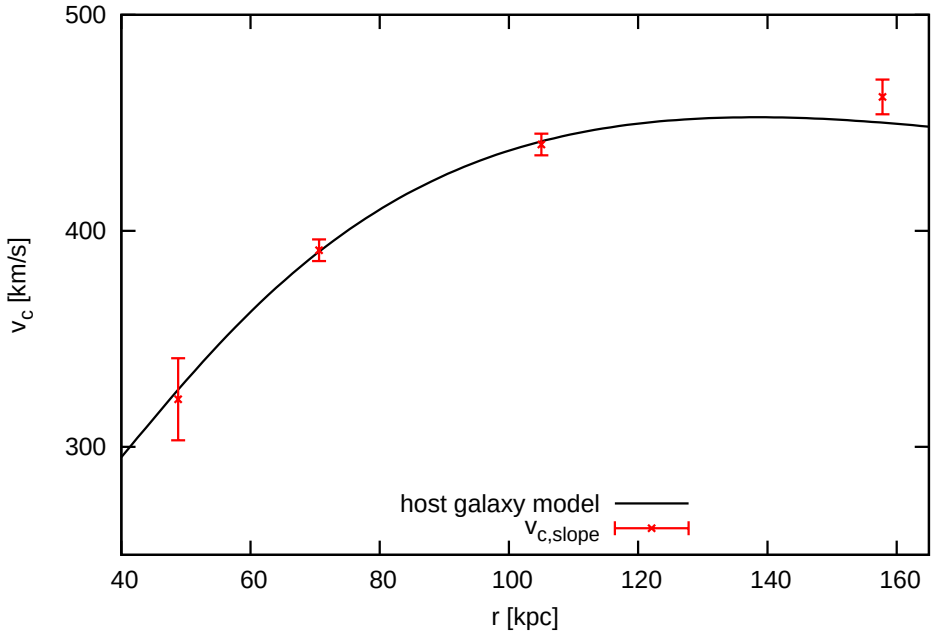


Figure 7: Circular velocity of the model (black curve) and values derived from the simulated data (red crosses).

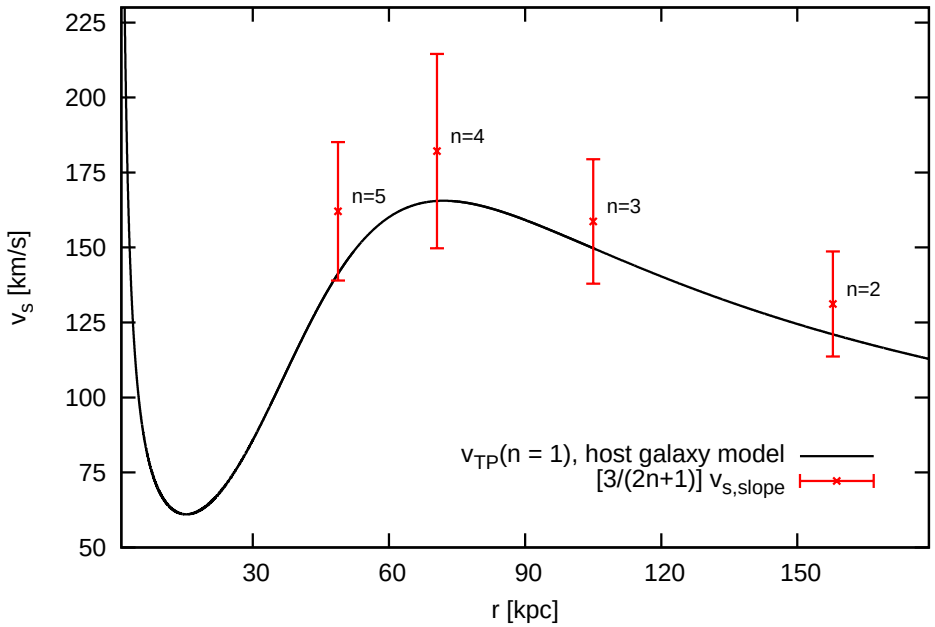


Figure 8: Comparison of velocity of the shell as a function of radius from the model and the simulated data. Velocity for the first shell ($n = 1$) in the host galaxy model is shown by the black curve. Red crosses show shell velocity as they result from the analysis of the simulated LOSVD. Values are corrected for shell number $n$.

Thus, we adopted the universal criteria: 1) the LOSVD of each shell is observed down to 0.9 times its radius; 2) we *measured* the positions of the LOSVD peaks in different locations within the shell, sampled by 1 kpc steps. These criteria give us between 7 and 15 *measurements* for a shell. Each *measurement* contains two values: the positions of the outer and inner peaks, $v_{\mathrm{los,max+}}$ and $v_{\mathrm{los,max-}}$, respectively, for each projected radius $R$ . We do not estimate the errors, since the real data will be dominated by other sources. We quote only the mean square deviation and the standard error of the linear regression.

We obtain the best agreement with the circular velocity of our host galaxy potential when using the slope of the LOSVD intensity maxima given by Eq. (3), where we fit the linear function of the *measured* distance between the outer and the inner peak on the projected radius, see Fig. 7. To estimate shell velocity, we use a hybrid relation Eq. (4) between the positions of the LOSVD peaks, the circular velocity at the shell edge radius $v_{\mathrm{c}}$, and the shell velocity. We substitute the values of the circular velocity derived from the *measurements* (that we know better describe the real circular velocity of host galaxy) into this relation, thus obtaining the improved *measured* shell velocity, see Fig. 8.

# 8 Dynamical friction and gradual disruption

This time, we will try to get closer to real shell galaxies by introducing into the test-particle simulations the gradual decay of the secondary galaxy as well as its braking by dynamical friction against the primary.

The dynamical friction is a braking force of gravitational origin, caused by the sole fact that the area, through which the secondary galaxy (or, in general, any object passing through a galaxy or another extended object) flies is not an empty space filled with a smooth potential, but a large sea of individual stars that are affected by gravity of the transiting object.

In test-particle simulations, the Chandrasekhar formula is commonly used to include dynamical friction. Its relative simplicity is made possible, among others, by the oversimplifying assumption of homogeneity of the stellar and dark matter distributions. To avoid it, we used the axial symmetry of our merger configuration to simplify the integrals over impact parameters and velocity distributions so that they can be solved numerically.

Together with the dynamical friction, the tidal disruption is another effect that is important for the galactic merger. The tidal disruption gradually lowers the mass of the cannibalized galaxy and thus mitigates the effect of the dynamical friction. During shell formation, it is of particular importance, because the gradual release of stars from the secondary galaxy has an important effect on the growing shell structure. The introduction of the tidal disruption into test-particle simulation is nevertheless a difficult task.

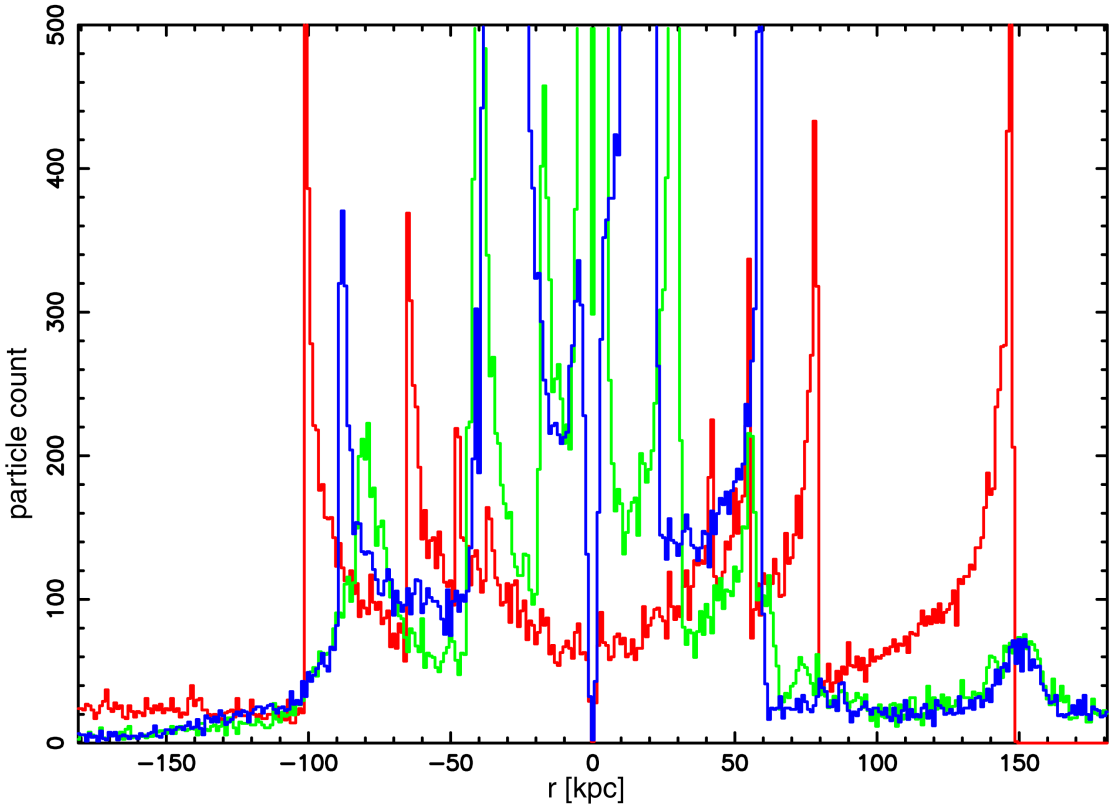


Figure 9: Radial histogram of stars of the secondary galaxy, centered on the primary 5 Gyr after the first passage of the secondary galaxy through the center of the primary galaxy for the three different simulations – run 1 (red), run 2 (green) and run 3 (blue).

Another thing going on during the merger that is difficult to reproduce in test-particle simulations is the deformation if the cannibalized galaxy. We model components of galaxies with spherically symmetric Plummer spheres. Thus we have tried at least to change the Plummer radius of the sphere of the secondary galaxy during the simulation according to the test particle distribution in each time step.

We have compared three simulations, all of them for the same set of parameters.

- Run 1 – without dynamical friction and with instant disruption of the secondary.
- Run 2 – dynamical friction is calculated using our modification of the Chandrasekhar's formula and the tidal disruption using the analytical approach based on the tidal radius as described at the beginning.
- Run 3 – dynamical friction is again calculated using our modification of the Chandrasekhar's formula, the tidal disruption is based on the counting of particles inside/outside the current tidal radius. Additionally, the Plummer radius of the secondary galaxy is constantly recalculated.

Radial histograms of particles in Fig. 9. The introduction of the dynamical friction and the gradual decay to our simulations dramatically changes the appearance of shell structures. While the position of the outermost shell is not much affected by the dynamical friction, its brightness is rapidly lowered due to the many particles staying trapped in the weakened but remaining potential of the small galaxy. The following shells are shifted and other generations of shells are added during next passages of the satellite through the center of the primary. Video from run 1 and run 2 is available at: galaxy.asu.cas.cz/∼ivaana/phd

Runs 2 & 3 are more consistent with observations in the sense that their contain shells on both small and large radii. An important thing to notice is that within our model, any subsequent passage of the secondary galaxy through the center of the primary galaxy does not lead to a complete destruction of the shells from the previous passages. Towards the center of the host galaxy, we find shells with larger surface brightness, also a feature found in real shell galaxies. At the same time, in Runs 2 & 3 we can find faint shells surrounded by brighter ones from both sides, another effect observed in real galaxies and impossible to reproduce in a simple simulation.

The main difference between Run 2 and Run 3 lies in the positions of the shells from the later generations – those shells that dominate the system in later times thanks to their brightness. The timing of the second passage of the secondary galaxy through the center of the host galaxy is very similar for Run 2 and Run 3 but the difference in energy, mass and decay of the secondary galaxy is sufficient to produce shells at different radii. Run 3 also differs significantly from Run 2 (and also Run 1) in that a bright shells system persist even a long time after the first approach of the secondary galaxy (7 Gyr). However, we cannot say whether it is Run 2 or Run 3 that better describes the real merger of two galaxies under given initial conditions. This indicates that quantitative modeling of a shell system using test-particle simulation is very difficult or even impossible.

In spite of the difficulties, we dare to state qualitative conclusions independently on the method chosen for the tidal decay of the secondary galaxy: the introduction of the dynamical friction and the gradual decay to our simulations dramatically changes the appearance of shell structures. Only the outermost shell of the first generation is not overlayed by later, brighter generations of shells added during next passages of the satellite through the center of the primary. While the position of the outermost shell is not much affected by the dynamical friction, its brightness is rapidly lowered due to the many particles staying trapped in the weakened but remaining potential of the small galaxy.

# 9 Discussion

We developed a new method to measure the potential of shell galaxies from kinematical data, extending the work of Merrifield & Kuijken (1998), assuming a constant shell phase velocity and a constant radial acceleration in the host galaxy potential for each shell. The best method for deriving the circular velocity in the potential of the host galaxy seems to be to use the slope of the LOSVD intensity maxima, Eq. (3), with a typical deviation in the order of units of km/s when fitting a linear function over all the measured positions of the LOSVD peaks for each shell. This circular velocity is then used in the hybrid relation, Eq. (4), to obtain the best estimate of the shell velocity.

However, derive a shell velocity systematically larger, 7–30%, than the real velocity is. That can be caused by nonradial trajectories of the stars of the cannibalized galaxy or by poor definition of the shell radius in the simulation. Nevertheless, the shell velocity depends, even in the simplified model of an instant decay of the cannibalized galaxy in a spherically symmetric host galaxy, on the serial number of the shell and on the whole potential from the center of the galaxy up to the shell radius. A comparison of its measured velocity to theoretical predictions is possible for a given model of the potential of the host galaxy and the presumed serial number of the observed shells. In such a case, however, it can be used to exclude some parameters or models of the potential that would otherwise fit the observed circular velocity.

The first shell has a serial number equal to one. A higher serial number means a younger shell. On the same radius, the velocity of each shell is always smaller than that of the previous one. In practice, it is difficult to establish whether the outermost observed shell is the first one created, or whether the first shell (or even the first couple of shells) is already unobservable. Here, we can use the potential derived from our method or a completely different one in a reverse way: to determine the velocity of the first shell on the given radius and to compare it to the velocity derived from the positions of the LOSVD peaks. Knowing the serial number of the outermost shell and its position allows us then to determine the time from the merger and the impact direction of the cannibalized galaxy. Moreover, the measurement of shell velocities can theoretically reveal the shells from different generations, which can be present in a shell galaxy (Bartošková et al., 2011).

Our method for measuring the potential of shell galaxies has several limitations. Theoretical analyses were conducted over spherically symmetric shells, while the test-particle simulation was run for a strictly radial merger and analyzed in a projection plane parallel to the axis of the merger. In addition, both analytical analyses and simulations assume spherical symmetry of the potential of the host galaxy. In reality, the regular shell systems with higher number of shells in a single host galaxy are more often connected to galaxies with significant ellipticity (Dupraz & Combes, 1986). Moreover, in cosmological simulations with cold dark matter, halos of galaxies are described as triaxial ellipsoids (e.g., Jing & Suto, 2002; Bailin & Steinmetz, 2005; Allgood et al., 2006). However, the effect of the ellipticity of the isophotes of the host

galaxy on the shell kinematics need not be dramatic, as the shells have the tendency to follow equipotentials that are in general less elliptical than the isophotes. Dupraz & Combes (1986) concluded that while the ellipticity of observed shells is generally low, it is neatly correlated to the eccentricity of the host galaxy. Our method is in principle applicable even to shells spread around the galactic center, which are usually connected to rounder elliptical galaxies if they were created in a close-to-radial merger. Nevertheless, the combination of the effects of the projection plane, merger axis, and ellipticity of the host galaxy can modify our results and require further analyses.

Another complication is that the spectral resolution required to distinguish all four peaks is probably quite high and the shell contrast is usually small. The higher order approximation is sensible only when kinematical data are available to larger distances from the shell edge. In the application to simulated data we considered a shell that is observable down to 0.9 shell radii. Nevertheless, there is the possibility to measure shell kinematics using the LOS velocities of individual globular clusters, planetary nebulae, and, in the Local group of galaxies, even of individual stars. It is even possible that the shell kinematics will be detectable in H I and CO emission.

The dynamical friction and gradual decay of the cannibalized galaxy has a dramatic influence on the resulting shell structure. Their implementation in test-particle simulations is a little involved. For the dynamical friction we used our own modification of the Chandrasekhar's formula for radial trajectories which is more faithful to the true stellar distribution function of the host galaxy. But when compared with the self-consistent simulations, our method is found to significantly overestimate the friction. Our simulations thus have to be understood as the upper estimate on the true effect of the dynamical friction on the shell formation.

To include the tidal disruption of the secondary galaxy in test-particle simulation is not less involved. We have tried several methods. Moreover we tried to reflect on the change of the shape of the gravitational potential of the cannibalized galaxy during the merger using a variable Plummer radius. The problem is that we have no hint as to which of the methods is a better approximation for the true decay of the secondary galaxy. If we were to compare the results with self-consistent simulations, we would likely get different results depending mainly on the configuration of the merger. Thus we have carried out several simulations using different methods for the decay of the secondary galaxy, focusing on qualitative effects in which these simulations differ from simple simulations that assume instantaneous breakdown of the secondary galaxy and no dynamical friction. We can believe that effects that are independent of the method used are more likely to participate in shell forming process in reality.

One such effect is that while the position of the outermost shells of the first generation is not much affected by the inclusion of the gradual decay and dynamical friction in the simulations, its brightness is drastically lowered. The same effect is observed in our self-consistent simulation. Even easily inferring the age of the collision is rendered impossible (as already pointed out by Dupraz & Combes, 1987). The shell systems in Fig. 9, all having the outermost shell at +150 kpc, are seen

5 Gyr after the first passage of the cannibalized galaxy through the center of the host galaxy. If we observationally identify the leftmost shell (around −80 kpc in Fig. 9) as being the outermost one, we would mistakenly estimate the merger age to be only ∼ 2.5 Gyr. We would also wrongly determine the direction from which the secondary galaxy came: assuming the classical picture (based on simulations without friction and with instantaneous disruption), the outermost shell would be located on the side from which the satellite came, so we would conclude it went from the left while the opposite is true.

Presence of a dark matter halo in the primary galaxy changes not only the dependence of the period of radial oscillations on radius, but also the range of stellar energies through the change of the velocity of the accreted satellite. The halo allows for a faster development of shells at larger radii. A more massive halo creates a larger range of shell radii in our simulations than a less massive one. The increased total mass of the host galaxy is more important than the difference in the dynamical friction caused by the differences in local density and velocity dispersion for different halo configurations. The more massive halo accelerates the secondary galaxy more, reducing the loss of its energy via the dynamical friction and increasing the time before a subsequent return of the secondary galaxy. The higher velocity of the secondary galaxy also means that the primary galaxy catches only very few particles in the first passage and a significant growth of the shell structure is observed only in later phases of the merger.

In general, it seems that test-particle simulations are not suitable for a quantitative reproduction of observed shell systems. There is no reliable (semi-)analytical method to calculate the dynamical friction in radial and close-to-radial minor mergers. Apparently even more importantly, there is no universal method to model the tidal decay of the cannibalized galaxy in test-particle simulations. Unfortunately, it turns out that it is exactly the details of the decay of the secondary galaxy that affect significantly the overall shell structure. In two simulations, with apparently small differences in the loss of mass and energy of the secondary galaxy during the first passage and the time of the second passage, shells of the second generations were created at different radii with respect to the shells from the first generation (which are otherwise very similar between the simulations). Moreover, the brightness of these shells differs and with each farther passage of the secondary galaxy, the difference in the appearance of the shell system increases and the observability of shells in the host galaxy changes by whole gigayears. Overall, an accurate reproduction of a shell galaxy is a very delicate matter, as in practice we do not know an exact distribution of mass in the host galaxy, the original trajectory of the secondary galaxy, nor its own mass distribution and our simulations suggest that the shell structure is very sensitive even to small details in these quantities.

Nevertheless even despite the simplicity of the models we used, it turned out that our test-particle simulations with gradual disruption and dynamical friction of the secondary galaxy do better than the simple simulations in reproducing observed features in real shell galaxies (range of shell radii, shell distribution, shell brightness distribution, etc.). We thus conclude that also in real galaxies, these features are the

result of combined effects of the gradual decay and dynamical friction.

At the end, we shall stress that while all these details have a large effect on the overall appearance of the shell system, they are not very important for the application of the method to measure the host galaxy potential from kinematical data. This method relies only on the assumption that the stars that form one particular shell are moving along radial trajectories and were released in the center of the primary galaxy together at some moment in the past. Within the framework the radial-minor-merger model, neither the gradual decay of the secondary galaxy nor the dynamical friction do not in principle have a large influence on the radiality of the stellar trajectories. Also, even when these effects are present, stars are being released in short time intervals when the secondary galaxy passes through the center of the primary galaxy, however these intervals are slightly larger than zero, which would be the case for the instantaneous decay of the secondary galaxy. This fact causes the shells to be slightly more diffuse and can interfere with an effort to determine the positions of the spectral peaks and the shell edge. Nevertheless, in principle the measurement of the potential should be still possible.

Ideally, for systems with multiple shells we would like to combine measurements of shell kinematics and their radial distribution, possibly also with measurements of surface brightness profile. The kinematical measurements supply us with the magnitude of acceleration at the shell edge and an estimate of the phase shell velocity, which allows us to separate the shells in different generations, if these are present. Simulations with the dynamical friction and gradual decay of the secondary galaxies that reproduce the kinematic and photometric data will then constrain other parameters of the merger such as its age and the trajectory and nature of the satellite galaxy. A similar result has been obtained for M31 (Fardal et al., 2012) whereas for the other shell galaxies, obtaining the kinematical data is a great challenge for the future generation of astronomical instruments.

# 10 Conclusions

Shells produced during nearly radial minor mergers of galaxies can be used probe the merger history of the host galaxy. We compared a simulation without dynamical friction and with instant disruption of the elliptical dwarf during the first passage through the center of a giant elliptical to a model with the same initial conditions but dynamical friction and gradual decay of the dwarf involved. It turns out that the resulting shell system is very sensitive to small differences during the decay of the cannibalized galaxy and thus the test-particle simulations are not suitable for a quantitative reproduction of observed shell systems. However these enhanced test-particle simulations do better than the simple simulations in reproducing observed features in real galaxies, including features that the simple simulations cannot show at all (range of shell radii, shell distribution, shell brightness distribution, etc.). We thus conclude that also in real galaxies, these features are the result of combined effects of the gradual decay and dynamical friction.

One effect found commonly in all the enhanced test-particle simulations is that while the position of the outermost shells of the first generation is not much affected by the inclusion of the gradual decay and dynamical friction in the simulations, its brightness is drastically lowered. The same effect is observed in our self-consistent simulation. Even just inferring the age of the collision is thus tricky: if we observationally miss the weakened outermost shell, which should be clearly visible according to simple simulations, we would underestimate the merger age by a factor of 2. At the same time, we would also wrongly determine the direction from which the secondary galaxy came.

On the other hand, kinematics of shells can be used to constrain their gravitational force field and thus the dark matter distribution. We show that line-of-sight velocity distribution of the shells has a quadruple-peaked shape. For spherical potential of the host galaxy and radial orbits of stars, we derive an analytical approximation, relating the circular velocity of the host galaxy potential at the shell edge radius, as well as the current phase velocity of the shell, to the positions of the four peaks. In galaxies with multiple shells, we can use circular velocities measured by these methods to determine the potential of the host galaxy over a large span in radii, whereas the measured shell phase velocity carries information on the age of the shell system, and the arrival direction of the cannibalized galaxy. The potential observation of multigeneration shell systems contains additional limits on the shape of the potential of the host galaxy.

The analytical expressions were applied to a test-particle simulation of a radial minor merger. The potential of the simulated host galaxy was successfully recovered. Shell kinematics can thus become an independent tool to determine the content and distribution of the dark matter in shell galaxies up to $\sim$100 kpc from the center of the host galaxy.

# References


Allgood, B., Flores, R. A., Primack, J. R., et al. 2006, MNRAS, 367, 1781

Arp, H. 1966a, Atlas of peculiar galaxies (Pasadena: California Inst. Tech., 1966)

Arp, H. 1966b, ApJS, 14, 1

Auger, M. W., Treu, T., Bolton, A. S., et al. 2010, ApJ, 724, 511

Bailin, J. & Steinmetz, M. 2005, ApJ, 627, 647

Balcells, M. 1997, ApJ, 486, L87

Balcells, M., van Gorkom, J. H., Sancisi, R., & del Burgo, C. 2001, AJ, 122, 1758

Bartošková, K., Jungwiert, B., Ebrová, I., Jílková, L., & Křížek, M. 2011, in Environment and the Formation of Galaxies: 30 Years Later, ed. I. Ferreras & A. Pasquali, 195–196

Canalizo, G., Bennert, N., Jungwiert, B., et al. 2007, ApJ, 669, 801

Carter, D., Allen, D. A., & Malin, D. F. 1982, Nature, 295, 126

Carter, D., Prieur, J. L., Wilkinson, A., Sparks, W. B., & Malin, D. F. 1988, MNRAS, 235, 813

Charmandaris, V., Combes, F., & van der Hulst, J. M. 2000, A&A, 356, L1

Churazov, E., Forman, W., Vikhlinin, A., et al. 2008, MNRAS, 388, 1062

Churazov, E., Tremaine, S., Forman, W., et al. 2010, MNRAS, 404, 1165

Coccato, L., Gerhard, O., Arnaboldi, M., et al. 2009, MNRAS, 394, 1249

Colbert, J. W., Mulchaey, J. S., & Zabludoff, A. I. 2001, AJ, 121, 808

Coleman, M., Da Costa, G. S., Bland-Hawthorn, J., et al. 2004, AJ, 127, 832

Das, P., Gerhard, O., Churazov, E., & Zhuravleva, I. 2010, MNRAS, 409, 1362

Deason, A. J., Belokurov, V., Evans, N. W., & McCarthy, I. G. 2012, ApJ, 748, 2

Dupraz, C. & Combes, F. 1986, A&A, 166, 53

Dupraz, C. & Combes, F. 1987, A&A, 185, L1

Ebrová, I., Jílková, L., Jungwiert, B., et al. 2012, A&A, 545, A33

Fardal, M. A., Guhathakurta, P., Gilbert, K. M., et al. 2012, MNRAS, 423, 3134

Forbes, D. A. 1992, PhD thesis, University of Cambridge

Fort, B. P., Prieur, J.-L., Carter, D., Meatheringham, S. J., & Vigroux, L. 1986, ApJ, 306, 110

Fukazawa, Y., Botoya-Nonesa, J. G., Pu, J., Ohto, A., & Kawano, N. 2006, ApJ, 636, 698

Hernquist, L. & Quinn, P. J. 1987a, ApJ, 312, 17

Hernquist, L. & Quinn, P. J. 1987b, ApJ, 312, 1

Horellou, C., Black, J. H., van Gorkom, J. H., et al. 2001, A&A, 376, 837

Jing, Y. P. & Suto, Y. 2002, ApJ, 574, 538

Kim, T., Sheth, K., Hinz, J. L., et al. 2012, ApJ, 753, 43

Koopmans, L. V. E., Bolton, A., Treu, T., et al. 2009, ApJ, 703, L51

Koopmans, L. V. E., Treu, T., Bolton, A. S., Burles, S., & Moustakas, L. A. 2006, ApJ, 649, 599

Liu, C. T., van Gorkom, J. H., Hibbard, J. E., Schiminovich, D., & Fujita, A. 1999, in Bulletin of the American Astronomical Society, Vol. 31, Bulletin of the American Astronomical Society, 833

Malin, D. F. & Carter, D. 1983, ApJ, 274, 534
Mandelbaum, R., Seljak, U., & Hirata, C. M. 2008, J. Cosmology Astropart. Phys., 8, 6
Martínez-Delgado, D., Gabany, R. J., Crawford, K., et al. 2010, AJ, 140, 962
McGaugh, S. S. & Bothun, G. D. 1990, AJ, 100, 1073
Merrifield, M. R. & Kuijken, K. 1998, MNRAS, 297, 1292
Nierenberg, A. M., Auger, M. W., Treu, T., Marshall, P. J., & Fassnacht, C. D. 2011, ApJ, 731, 44
Norris, M. A., Gebhardt, K., Sharples, R. M., et al. 2012, MNRAS, 421, 1485
Nulsen, P. E. J. 1989, ApJ, 346, 690
Petric, A., Schiminovich, D., van Gorkom, J., van der Hulst, J. M., & Weil, M. 1997, in Bulletin of the American Astronomical Society, Vol. 29, Bulletin of the American Astronomical Society, 1344
Pierfederici, F. & Rampazzo, R. 2004, Astronomische Nachrichten, 325, 359
Prieur, J.-L. 1988, ApJ, 326, 596
Prieur, J.-L. 1990, in Dynamics and Interactions of Galaxies, ed. R. Wielen, 72–83
Quinn, P. J. 1984, ApJ, 279, 596
Rampazzo, R., Marino, A., Tantalo, R., et al. 2007, MNRAS, 381, 245
Reduzzi, L., Longhetti, M., & Rampazzo, R. 1996, MNRAS, 282, 149
Ryan, Jr., R. E., Cohen, S. H., Windhorst, R. A., & Silk, J. 2008, ApJ, 678, 751
Schiminovich, D., van Gorkom, J., van der Hulst, T., Oosterloo, T., & Wilkinson, A. 1997, in Astronomical Society of the Pacific Conference Series, Vol. 116, The Nature of Elliptical Galaxies; 2nd Stromlo Symposium, ed. M. Arnaboldi, G. S. Da Costa, & P. Saha, 362–363
Schiminovich, D., van Gorkom, J. H., van der Hulst, J. M., & Kasow, S. 1994, ApJ, 423, L101
Schiminovich, D., van Gorkom, J. H., van der Hulst, J. M., & Malin, D. F. 1995, ApJ, 444, L77
Schweizer, F. 1983, in IAU Symposium, Vol. 100, Internal Kinematics and Dynamics of Galaxies, ed. E. Athanassoula, 319–326
Schweizer, F. & Ford, Jr., W. K. 1985, in Lecture Notes in Physics, Berlin Springer Verlag, Vol. 232, New Aspects of Galaxy Photometry, ed. J.-L. Nieto, 145–150
Schweizer, F. & Seitzer, P. 1988, ApJ, 328, 88
Sikkema, G., Carter, D., Peletier, R. F., et al. 2007, A&A, 467, 1011
Springel, V., Di Matteo, T., & Hernquist, L. 2005, MNRAS, 361, 776
Tal, T., van Dokkum, P. G., Nelan, J., & Bezanson, R. 2009, AJ, 138, 1417
Thomas, J., Saglia, R. P., Bender, R., et al. 2011, MNRAS, 415, 545
Turnbull, A. J., Bridges, T. J., & Carter, D. 1999, MNRAS, 307, 967
Weijmans, A.-M., Krajnović, D., van de Ven, G., et al. 2008, MNRAS, 383, 1343
Wilkinson, A., Browne, I. W. A., Kotanyi, C., et al. 1987a, MNRAS, 224, 895
Wilkinson, A., Browne, I. W. A., & Wolstencroft, R. D. 1987b, MNRAS, 228, 933
Wilkinson, A., Sparks, W. B., Carter, D., & Malin, D. A. 1987c, in IAU Symposium, Vol. 127, Structure and Dynamics of Elliptical Galaxies, ed. P. T. de Zeeuw, 465–466

# List of publications

I. Ebrová, L. Jílková, B. Jungwiert, M. Křížek, M. Bílek, K. Bartošková, T. Skalická, and I. Stoklasová, 2012, *Quadruple-peaked spectral line profiles as a tool to constrain gravitational potential of shell galaxies*, Astronomy & Astrophysics, Volume 545, id.A33

M. Bílek, B. Jungwiert, L. Jílková, I. Ebrová, K. Bartošková, and M. Křížek, 2013, *Testing MOND gravity in the shell galaxy NGC 3923*, accepted for publication in Astronomy & Astrophysics

I. Ebrová, L. Jílková, B. Jungwiert, K. Bartošková, M. Křížek, T. Bartáková and I. Stoklasová, 2011, *Quadruple-Peaked Line-of-Sight Velocity Distributions in Shell Galaxies*, Environment and the Formation of Galaxies: 30 years later Astrophysics and Space Science Proceedings 2011, pp 225-227

I. Ebrová, K. Bartošková, B. Jungwiert, L. Jílková, M. Křížek, 2011, *Comparing Various Approaches to Simulating the Formation of Shell Galaxies*, Environment and the Formation of Galaxies: 30 years later Astrophysics and Space Science Proceedings 2011, pp 199-201

I. Ebrová, B. Jungwiert, G. Canalizo, N. Bennert, L. Jílková, 2010, *Shell Galaxies: Dynamical Friction, Gradual Satellite Decay and Merger Dating*, Galaxy Wars: Stellar Populations and Star Formation in Interacting Galaxies ASP Conference Series Vol. 423, proceedings of a conference held 19-22 July 2009 at East Tennessee State University, Johnson City, Tennessee, USA. Edited by Beverly Smith, Nate Bastian, Sarah J. U. Higdon, and James L. Higdon. San Francisco: Astronomical Society of the Pacific, 2010., p.236

I. Ebrová, B. Jungwiert, G. Canalizo, N. Bennert, L. Jílková, 2010, Shell Galaxies, *Dynamical Friction, and Dwarf Disruption*, Galaxies in Isolation: Exploring Nature Versus Nurture, proceedings of a conference held 12 to 15 May 2009 in Granada, Spain. Edited by Lourdes Verdes-Montenegro, Ascencíon del Olmo, and Jack Sulentic. San Francisco: Astronomical Society of the Pacific, 2010., p.252

K. Bartošková, B. Jungwiert, I. Ebrová, L. Jílková, M. Křížek, 2011, *Simulations of Shell Galaxies with GADGET-2: Multi-Generation Shell Systems*, Environment and the Formation of Galaxies: 30 years later Astrophysics and Space Science Proceedings 2011, pp 195-197

L. Jílková, B. Jungwiert, M. Křížek, I. Ebrová, I. Stoklasová, T. Bartáková, K. Bartošková, 2010, *Simulations of Line Profile Structure in Shell Galaxies*, Galaxy Wars: Stellar Populations and Star Formation in Interacting Galaxies ASP Conference Series Vol. 423, proceedings of a conference held 19-22 July 2009 at East Tennessee State University, Johnson City, Tennessee, USA. Edited by Beverly Smith, Nate Bastian, Sarah J. U. Higdon, and James L. Higdon. San Francisco: Astronomical Society of the Pacific, 2010., p.243